ANALES DE LA
Academia de Ciencias de Cuba

SECCIÓN CIENCIAS BIOMÉDICAS

Artículo original de investigación

Bioelectrical parameters estimated in newly diagnosed lung cancer patients with multifrequency-bioelectrical impedance

Dunia Rodríguez-Heredia [1] https://orcid.org/0000-0003-4676-7314
Arnolis Poll-Fernández [2] https://orcid.org/0000-0001-7078-921y
Maylet Planas-Rodríguez [3] https://orcid.org/0000-0002-0491-3793
Henry Bory-Prevez [4] https://orcid.org/0000-0001-5508-0501
Justa Carmen Columbié-Regüeiferos [5] https://orcid.org/0009-0003-6670-4414
Luis Enrique Bergues Cabrales [6*] https://orcid.org/0000-0001-8094-392X

[1] *Universidad de Oriente. Santiago de Cuba, Cuba*
[2] *Hospital General Docente Clínico Quirúrgico Dr. Agostinho Neto. Guantánamo, Cuba*
[3] *Universidad de Ciencias Médicas. Santiago de Cuba, Cuba*
[4] *Universidad de Oriente. Santiago de Cuba, Cuba*
[5] *Centro de Toxicología y Biomedicina. Santiago de Cuba, Cuba*
[6] *Centro Nacional de Electromagnetismo Aplicado, Universidad de Oriente. Santiago de Cuba, Cuba*

**Autor para la correspondencia:* berguesc@yahoo.com

Editor
Lisset González Navarro
Academia de Ciencias de Cuba.
La Habana, Cuba

Translator
Darwin A. Arduengo García
Academia de Ciencias de Cuba.
La Habana, Cuba

ABSTRACT

Introduction: The bioelectrical impedance analysis is used for the evaluation and monitoring in cancer patients. **Objective:** To estimate whole bioelectrical parameters obtained from the Cole-Cole distribution function with multifrequency-bioelectrical impedance analysis in newly diagnosed lung cancer adult patients. **Methods**: A pilot, prospective and cross-sectional study was carried out to measure the bioelectrical parameters with multi-frequency Bioelectrical Impedance Analysis (at 5, 50, 100 and 200) kHz in 23 newly diagnosed lung cancer adult patients. The Cole-Cole distribution function was used to estimate electrical resistance, capacitive reactance and impedance modulus between 100 Hz and 10 GHz. **Results**: Differences between the simulated and experimental data (electrical impedance modulus > 10 Ω) were observed in seven lung cancer patients at 100 and 200 kHz. Cole-Cole distribution function underestimated experimental data in the majority of these patients at (5, 50 and 100) kHz, not so at 200 kHz. The intracellular resistance was higher than extracellular resistance in all of them, in contrast with physiology. Furthermore, the overall cellular capacitance of cellular membrane in each lung cancer patient increased respect to that in apparently healthy subjects. **Conclusions**: The bioelectrical impedance analysis reveals anomalous behaviors of bioelectrical parameters in each newly diagnosed lung cancer adult patients for frequencies above characteristic frequency. These behaviors may be described by distribution functions Cole-Cole (for $0 < \alpha < 1$) or others.

Keywords: bioelectrical impedance; lung cancer; Cole-Cole model; electrical resistance

Parámetros bioeléctricos estimados en pacientes con cáncer de pulmón recientemente diagnosticados con impedancia bioeléctrica multifrecuencia

RESUMEN

Introducción: El análisis de impedancia bioeléctrica se usa para la evaluación y seguimiento de pacientes con cáncer. **Objetivo:** Estimar parámetros bioeléctricos corporales obtenidos a partir de la función de distribución Cole-Cole con el análisis de la impedancia bioeléctrica multifrecuencia en pacientes con cáncer de pulmón recientemente diagnosticados. **Métodos**: Se llevó a cabo un estudio piloto, prospectivo y transversal para medir los parámetros bioeléctricos con análisis de impedancia bioeléctrica multifrecuencia (a 5; 50; 100 y 200) kHz en 23 pacientes adultos con cáncer de pulmón de reciente diagnóstico. Se utilizó la función de distribución Cole-Cole para estimar la resistencia eléctrica, la reactancia capacitiva y el módulo de impedancia entre 100 Hz y 10 GHz. **Resultados**: Se observaron diferencias entre los datos simulados y experimentales (módulo de impedancia eléctrica mayor que10 Ω) en siete pacientes con cáncer de pulmón a 100 kHz y 200 kHz. La función de distribución Cole-Cole subestimó datos experimentales en la mayoría de estos pacientes a (5; 50 y 100) kHz, no así a 200 kHz. La resistencia intracelular fue mayor que la extracelular en todos ellos, en contraste con la fisiología. Además, la capacitancia celular de la membrana celular en cada paciente con cáncer de pulmón aumentó con respecto a la de los sujetos aparentemente sanos. **Conclusiones**: El análisis de impedancia bioeléctrica revela comportamientos anómalos de parámetros bioeléctricos en cada paciente adulto con cáncer de pulmón de reciente diagnóstico para frecuencias mayores a la característica. Estos comportamientos pueden ser descritos con funciones de distribución Cole-Cole (para $0 < \alpha < 1$) u otras.

Palabras clave: impedancia bioeléctrica; cáncer de pulmón; modelo de Cole-Cole; resistencia eléctrica

INTRODUCTION

The lung cancer is the first cause of death of all types of cancer worldwide and in Cuba. [1] The Bioelectrical Impedance Analysis (BIA) is used in cancer patients, specifically in lung cancer patients (LCPs) because changes in bioelectrical parameter are primary to biological and clinical ones. [1,2,3] Therefore, many researchers focus in cancer electrical properties (electrical conductivity and electrical permittivity), its active bioelectricity and bioelectronic (faradic and ionic currents), and surface charge density on tumor-healthy tissue boundary. [4,5,6,7] Electrical alterations in cancer have been related to its altered metabolism and biological characteristics with respect to those in the surrounding healthy tissue. [6,8,9] Additionally, BIA allows estimating body water and its compartments, body composition and nutritional status and other parameters from the estimation of body bioelectrical parameters in apparently healthy adult subjects (AHASs), cancer patients and other pathologies. [9,4,5,10,11,2,3,11)

Columbié-Regüeiferos et al. [1] report a pioneering study that integrates tumor and patient variables (clinical, bioelectrical and functional) and the Principal Component Analysis in newly diagnosed lung cancer adult patients (NDLCAPs). As NDLCAPs are complex, open and nonlinear systems, knowledge of their initial variables is essential because cancer patients may evolve unfavorably for small changes in at least one of these initial parameters. Consequently, an unfavorable forecast of NDLCAPs is expected a posteriori. [12,13,1] That is why, we focus in to characterize NDLCAPs by means of BIA.

Columbié-Regüeiferos et al. [1] report bioelectrical parameters at 50 kHz in NDLCAPs; nevertheless, they do not report these parameters and others at different frequencies. Furthermore, parameters of Cole-Cole distribution functions in NDLCAPs are not documented in the literature. Therefore, the objective of this study is to estimate whole bioelectrical parameters obtained from the Cole-Cole distribution function with multifrequency-BIA in NDLCAPs.

METHODS

Ethic aspects

A pilot, prospective and cross-sectional study was carried out at the Pneumology Service of the Hospital General Dr. Juan Bruno Zayas Alfonso, Santiago de Cuba, Cuba (from March 1 to September 30, 2018). This study was approved by the Ethics Committee (Current Controlled trials BIACANCER108823SC900-149; May 5, 2017) and the Scientific Council (Resolution 189/2017; June 7, 2017) of this hospital, and governed by the ethical standards of the Declaration of the Helsinki World Medical Assembly. [14] Name of the register of this Pilot study is BIACANCER and its registration data is December 6, 2017 at the Universidad de Ciencias Médicas, Santiago de Cuba, Cuba. Date of enrolment of the first participant in this Pilot study is March 1, 2018. Furthermore, this research is fulfilled with good medical clinical practices established by the Ministry of Health of the Republic of Cuba. [15]

NDLCAPs were included in this Pilot study once they, their companion and witness (psychologist) proceeded to the reading, agreement, and signature of the Informed Consent. They received previously a detailed explanation of objectives, importance and purposes of this study, and requirements established for measurements (empty bladder, no smoking at least 24 h prior, no intake of steroids at least one week before, no intake of water and alcoholic beverages at least 24 h prior, fasting 2 h minimum, and non-performance of physical exercises 12 h before taking measurements).

Patients

The personal history of each NDLCAPs was collected. The inclusion criteria were the Informed Consent signed and approved, lung cancer cyto-pathological diagnosis and NDLCAPs received medical attention at the Pneumology Service. Exclusion criteria were patient and family refusals to participate in this study, patients with metallic implants in the body, amputated limbs, generalized skin diseases, serious infections, and disorders of body fluids. Voluntary abandonment and death were established as exit criteria. In this study 23 NDLCAPs participated [aged (53-82) years: 14 men and 9 women]. A numerical code (from 1 to 23) was assigned to each patient in order of arrival. [1]

Columbié-Regüeiferos et al. [1] reported the age, gender, height (H), unintentional patient body weight, relative change in unintentional body weight (ΔP), degree of ECOG functional scale, (Eastern Cooperative Oncology Group) lung cancer stage, the lung cancer histological varieties for each NDLCAPs and men/women ratio. They analyzed the prevalence of these variables and explained them. Therefore, these results were not shown in this study, but used to explain anomalies in bioelectrical parameters of NDLCAPs.

Electric bioimpedance analyzer

The Bodystat Quadscan® 4000 multi-frequency BIA analyzer (company Bodystat, LTD, Douglas Isle of Man, British Isles, available at https://www.bodystat.com/) was used to estimate the body electrical impedance modulus (|Z| in Ω) at (5, 50, 100 and 200) kHz, named |Z| 5 kHz, |Z| 50 kHz, |Z| 100 kHz, and |Z| 200 kHz, respectively. The body electrical resistance, R (in Ω), at 50 kHz (R 50 kHz); body electrical reactance module, |*Xc*| (in Ω), at 50 kHz |*Xc*| 50 kHz; and body phase angle module, |*θ*| (in °), at 50 kHz (|*θ*| 50 kHz) were also measured. These body bioelectrical parameters were interrelated by the following expressions (1)

$$|Z| = \sqrt{R^2 + |X_c|^2} \cdot \text{and} \cdot |\theta| = tg^{-1}(|X_c|/R) \quad (1)$$

Although |Xc| and |θ| were used in this study, |Xc| and |θ| were strictly negative because tissues in NDLCAPs were purely considered resistive-capacitive (inductive effects in human body were neglected). [1] Nevertheless, inductive effects were reported in AHASs. [16] The calibrator supplied by the manufacturer 500.0 (± 0.1) Ω allowed evaluating the stability of the Bodystat Quadscan® 4000 multi-frequency BIA analyzer at the beginning and the end of the measurement in each patient. The values of $R_{50\,kHz}$ /height, $|Xc|_{50\,kHz}$ /height and $|\theta|_{50\,kHz}$ in male and female NDLCAPs were compared with their respective normal intervals reported in AHASs (2-80) years living in Santiago de Cuba, Cuba, specifically those in the age range (50-80) years in both genders. [17]

Measurement procedure

The standardized procedure for measurement R and |*Xc*| was the same reported in Regüeiferos JCC et al Lafargue AL et al. [1,16] Height (nearest 0.5 cm with the technique of the International Biological Program with the head located in the Frankfort plane, precision ± 0.1 cm), body weight (Soehnle Professional digital scale, model 2755, Soehnle Industrial Solution, Backnany, Germany, accuracy of ± 0.5 kg) and BIA parameters (from 8 to 9 am) in NDLCAPs were measured in this study. Furthermore, it was considered controlled environmental conditions: temperature of 25 (± 1)°C (Sattigungs thermometer of precision ± 1°C, Germany), relative humidity of 60 (± 5)% (Fischer Polymeter of precision ± 1%, Germany) and neutral (environment free of field generating equipment and electromagnetic radiation).

The NDLCAPs were covered with light clothing and placed in a supine position on a non-conductor surface, without a pillow under the head, with the arms separated at approximately 30° from the thorax and the legs separated approximately at an angle of 45° without contact between them. The skin of each patient was first cleaned with water and soap, and then 70% alcohol to ensure asepsis of the areas where the electrodes were attached. [1,16]

The right tetrapolar ipsilateral method was used. The injection electrodes of alternating electric current were placed in the medial areas of the dorsal surfaces of hands and feet, near the metacarpal and metatarsal phalangeal joints, respectively. The receiving electrodes of the body electrical voltage were placed between the distal epiphyses of the radius and the ulna, at the level of the pisiform eminence, as well as at the midpoint between both malleoli, respectively. The distance between the sensing and stimulating electrodes was 5.0 cm and measured with a standard measuring tape (model RT-144, Wintape Measuring Tape Co., Ltd, Guangdong, China) of 0.1 cm precision. Electrocardiogram electrodes (model APR-020, All Pro Corporation Company, Quingdao, China) were used. The material of each electrode was Silver/Silver Chloride (Ag/AgCl). [1,16]

Cole-Cole distribution function

Cole-Cole distribution function was used and given by (equation 2)

$$Z(f) = R_\infty + \frac{R_0 - R_\infty}{1 + \left(j\frac{f}{f_c}\right)^{1-\alpha}}, \quad (2)$$

where (in Hz), f_c (in Hz), *Z(f)* (in Ω), R_0 (in Ω), R_∞ (in Ω), α, and *j* were the frequency, characteristic frequency, electrical impedance in function of *f*, electrical resistance in low frequency, electrical resistance in high frequency, dimensionless exponent parameter related to tissue heterogeneity, and imaginary unit ($j^2 = -1$), respectively. The inverse of f_c was the relaxation time. The parameter α varied between 0 (tissue homogeneous) and 1 (tissue most heterogeneous). [18] In this study, α = 1 because NDLCAPs were considered very heterogeneous systems, in which were involved biophysical-chemical-metabolic alterations and relaxation phenomena (β-dispersion, from a few kHz up to a few dozen MHz, caused by the Maxwell-Wagner effect and sample type-dependent). [1,19]

The parameters R_0, R_∞, and f_c were obtained fitting of experimental data of *Z*(*f*) versus *f* plot with the nonlinear least square method and related to the electrical resistance of intercellular fluid (R_i, in Ω), electrical resistance of extracellular fluid (R_e, in Ω) and overall cellular capacitance of cellular membrane (C_m, in F), given by (equation 3, 4 y 5)

The parameter in Eq. (5) was obtained when |*Xc*| reached its maximum value |*Xc*| max. Eqs. (2)-(5) assumed that the entire assembly of the cell membrane was formed by the intercellular fluid, plasma membrane and extracellular fluid formed a conductor-dielectric-conductor like structure behaving as a parallel flat plate capacitor (figure 1A), whose equivalent electrical circuit was represented in figure 1B. [19]

As the bioelectrical parameters of cancer, respect to those of normal tissue, prevailed in the body bioelectrical parameters measured in cancer patients, Ri, Re, Cm and fc were mainly attributed to cancer. [1]

As experimental values of |Z| were reported only at (5, 50, 100 and 200) kHz, the Cole-Cole plot could not be done. Consequently, the Cole-Cole distribution function was not used to fit it. Despite, this plot for each NDLCAPs was made from the analysis and resolution of the equivalent electrical circuit (figure 1 B) to calculate any value of |*Z*|, R, |*Xc*| and |*θ*| in the range of 100 Hz ($f = f_0$) to 10 GHz ($f = f_\infty$), named simulated data. The values of |*Z*|, R, |*Xc*| and |*θ*|, at 100 Hz were named $|Z|_{100\ Hz}$, $R_{100\ Hz}$, $|Xc|_{100\ Hz}$ and $|\theta|_{100\ Hz}$, respectively, whereas at 10 GHz were named $|Z|_{10\ Hz}$, $R_{10\ Hz}$, $|Xc|_{10\ Hz}$ and $|\theta|_{10\ Hz}$, and for each NDLCAPs.

The difference between experimental and simulated data, named Δ|Z| (Δ|Z| = |Z| sim) was calculated at each discrete value of frequency (5, 50, 100 and 200) kHz for each NDLCAPs, where |Z|sim and |Z|exp were the body electrical impedance modules estimated with the interpolation of Cole-Cole distribution function and the Bodystat Quadscan® 4000 multi-frequency analyzer, respectively Δ|Z|. < 0 Ω (Δ|Z| > 0 Ω) meant that the Cole-Cole distribution function underestimated (overestimated) experimental data. Furthermore, a good agreement between |Z|sim and |Z|exp data was established when the modulus of Δ|Z|, named |Δ|Z|| was ≤ 10 Ω (associated to total body water ≤ 0.5 L, which had no clinical significance). [1]

$$R_e = R_0,$$
$$R_i = \frac{R_0 \cdot R_\infty}{R_0 - R_\infty},$$
$$C_m = \frac{R_0 R_\infty}{2\pi f_c R_0^2} = \frac{1}{2\pi f_c (R_i + R_e)}. \quad (3,4,5)$$

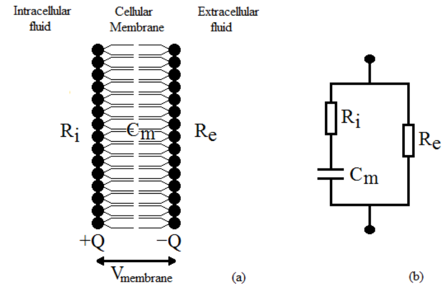

Fig. 1. Cell membrane model. A) Entire assembly; B) equivalent electrical circuit

As Δ|Z| was a measure of how much |Z|sim differed from |Z|exp at each frequency, the root means square value (RMS Δ|Z|, in Ω) was proposed to know the standard deviation of a set of Δ|Z| values over the whole frequency range of 5 to 200 kHz for each NDLCAPs. The set of Δ|Z| values were those computed at (5, 50, 100 and 200) kHz and RMS Δ|Z| was given by (6)

Although results were not shown, |Z| versus *f*, *R* versus *f*, |*X*c| versus *f*, |*θ*| versus *f*, |*X*c| versus R (Cole-Cole diagram) plots were done for each NDLCAPs, where f was varied from 100 Hz up to 10 GHz.

The values of R_e, R_i, C_m, fc, $R_{f\,c}$ and |*X*c|max were estimated from |Z|5 kHz, $|Z|_{50\ kHz}$, $|Z|_{100\ kHz}$, and $|Z|_{200\ kHz}$ values for each NDLCAPs, where R_f c and $|Xc|_{max}$ were R and |*X*c|maximum values at f_c, respectively. For this, it was solved a system of three equations with three unknown variables (R_e, R_i and C_m). These equations resulted from the resolution of the simplified Cole-Cole equivalent electrical circuit (figure 1B). The value of fc was calculated with Equation (5) once R_e, R_i and C_m were calculated. Furthermore, the modulus of impedance at *fc* (|Z| f_c, in Ω) was estimated from R_f c and $|Xc|_{max}$ values for each NDLCAPs.

The average and standard deviation (SD) of $|Z|_{100\ kHz}$, $R_{100\ kHz}$, $|Xc|_{100\ kHz}$ and $|\theta|_{100\ kHz}$, $|Z|_{5\ kHz}$, $|Z|_{50\ kHz}$, $R_{50\ kHz}$, $|Xc|_{50\ kHz}$ and $|\theta|_{50\ kHz}$, $|Z|_{100\ kHz}$, $|Z|_{200\ kHz}$, $|Z|_{10\ GHz}$, $|Z|_{50\ kHz}$, $R_{10\ GHz}$, $|Xc|_{10\ GHz}$ and $|\theta|_{10\ GHz}$, R_e, R_i, C_m, f_c, R_{fc}, $|Xc|_{max}$ and $|Z|_{fc}$, were calculated from their respective individual values.

Information processing

The original database was presented in tables, created in .txt for information processing, and guarded for 15 years in the Pneumology Service of the Hospital General Dr. Juan Bruno Zayas Alfonso. A computer program was implemented in GNU Octave 4.0 (free software, License 2015-05-29, Universidad de Oriente, Santiago de Cuba, Cuba) to fitting data with Equation(1) and showed figures of versus for each NDLCAPs. As part of the GNU Project, GNU Octave was free software under the terms of the GNU General Public License. The website was http://gnu.org/software/octave. Free Software Foundation funds the GNU Project. Developer(s): John W. Eaton and many collaborators. This software was executed in a 256-core processor HPC with 256 GB RAM. The duration of the processing of all data and graphs was approximately 1 min.

RESULTS

The table 1 shows the original experimental values of $R_{50\ kHz}$, $|Xc|_{50\ kHz}$, $|\theta|_{50\ kHz}$, $|Z|_{5\ kHz}$, $|Z|_{50\ kHz}$, $|Z|_{100\ kHz}$ and $|Z|_{200\ kHz}$ and their respective average and SD. The complete population of NDLCAPs had an average value $|\theta|_{50\ kHz}$ close to 6.0°. Nevertheless, the individual analysis revealed that 30.4% (7/23), 30.4% (7/23) and 39.2% (9/23) of them had values of $|\theta|_{50\ kHz}$ below, in normal range and above, respectively, respect to those in AHASs. [17] The examination by gender in NDLCAPs showed that the average ± SD of |*θ*|50 kHz were 6.2 ± 0.3 and 6.0 ± 0.8 in nine women and 14 men NDLCAPs, respectively. Furthermore, the analysis by gender and age groups indicated that the mean ± SD of $|\theta|_{50\ kHz}$ was 5.8 (± 0.4) for three women with ages < 60 years, 5.9 (± 0.9) for six women with ages ≥ 60 years, 6.3 (± 0.6)° for five men with ages < 60 years, and 5.8 (± 0.9)° for nine men with ages ≥ 60 years (table 1).

The |Z| decreased when increased in nine NDLCAPs; nevertheless, an anomalous behavior in |Z| was observed at 100 kHz (NDLCAPs with codes 7, 9, 12, 14, 17, 19 and 21) and 200 kHz (NDLCAPs with codes 10, 11, 13, 15, 18, 20 and 22). Consequently, deformation of the semicircle was revealed in the plot of |*X*c| versus of these 14 NDLCAPs for *f* > *fc*. Despite,

$$RMS_{\Delta|Z|} = \sqrt{\frac{1}{4}\sum_{f_i=1}^{4}\left(\Delta|Z|_{f_i}\right)^2}, \qquad (f_i = 5, 50, 100, 200\ kHz) \qquad (6)$$

Table 1. Body bioelectrical parameters

Patient code	*R50kHz* (Ω)	*|Xc|50kHz* (Ω)	*|ϑ|50kHz* (o)	*|Z|5kHz* (Ω)	*|Z|50kHz* (Ω)	*|Z|100kHz* (Ω)	*|Z|200kHz* (Ω)
1	403	48.9	6.7	433	416	391	369
2	402	42.9	6.1	459	404	382	362
3	610	44.3	4.2	667	611	588	569
4	465	43.0	5.3	520	467	444	426
5	478	21.7	3.6	500	479	467	454
6	523	56.6	6.2	600	526	496	472
7	404	51.4	6.6	515	446	531	397
8	561	65.9	6.7	652	565	528	503
9	556	59.2	6.1	638	559	664	509
10	693	50.6	5.3	789	696	578	664
11	571	49.4	6.7	676	601	393	566
12	566	48.4	6.2	466	412	578	368
13	514	44.3	6.3	663	609	494	553
14	521	43.2	6.2	599	524	538	462
15	513	44.8	6.2	648	569	382	513
16	557	51.8	6.3	443	403	393	362
17	558	50.7	6.1	437	418	657	367
18	611	45.4	5.3	762	687	540	633
19	558	47.3	6.1	598	560	657	521
20	640	60.3	5.9	761	688	531	634
21	527	57.4	5.8	641	561	589	501
22	572	50.9	6.2	612	603	419	573
23	568	52.3	6.4	463	436	420	413
Average	538.0	49.2	5.9	589.0	532.0	507.0	487.0
Standard deviation	72.7	8.6	0.8	110.1	95.3	92.6	94.1

Note: R_{50kHz}, $|X_c|_{50kHz}$, $|\theta|_{50kHz}$, $|Z|_{5kHz}$, $|Z|_{50kHz}$, $|Z|_{100kHz}$ and $|Z|_{200kHz}$ were defined in Material and Methods section.

the average values of $|Z|_{5\,kHz}$, $|Z|_{50\,kHz}$, $|Z|_{100\,kHz}$ and $|Z|_{200\,kHz}$ satisficed that |Z| decreased when f increased (table 1).

The simulated values of $|Z|_{100\,kHz}$, $R_{100\,kHz}$, $|Xc|_{100\,kHz}$, $|\theta|_{100\,kHz}$, $|Z|_{10\,kHz}$, $R_{10\,GHz}$, $|Xc|_{10\,kHz}$ and $|\theta|_{10\,kHz}$, were showed in table 2, which revealed that and values coincided with those of $|Z|_{5\,kHz}$ and $|Z|_{200\,kHz}$ estimated with BIA analyzer, respectively. The values of $|Z|_{exp}$, $|Z|_{sim}$, and Δ|Z| at 5, 50, 100 and 200 kHz are shown in table 3.

Tables 2 and 3 demonstrate that |Z| decreased as increased in the range of 100 Hz to 10 GHz. This was observed for all NDLCAPs, except those with codes 14 and 23, in which |Z| increased at 200 kHz (table 3). Table 3 revealed from the individual analysis of each NDLCAPs that the Cole-Cole distribution function underestimated |Z| at 5 kHz (in all patients), 50 kHz (eight NDLCAPs), 100 kHz (15 NDLCAPs) and 200 kHz (one patient). This distribution function overestimated |Z| in the rest of NDLCAPs at 50 kHz (15 NDLCAPs), 100 kHz (8 NDLCAPs) and 200 kHz (22 patients). Larges differences between the simulated and experimental data (Δ|Z|| > 10 Ω) were observed at 50 kHz (one patient), 100 kHz (17 patients and 200 kHz (three patients). These larges differences were not observed for Δ|Z|| at 5, 50, 100 and 200 kHz. Three patients had Δ|Z|| > 10 Ω in more than one frequency, as in NDLCAPs with code 8 (at 50, 100 and 200) kHz, and Codes 14 and 17 (at 100 and 200 kHz). Furthermore, values of RMS Δ|Z| greater than 10 Ω were observed in 17 NDLCAPs (codes 7-23) in the frequency range 5-200 kHz.

The Table 4 shows the individual values of R_e, R_i, C_m, f_c, R_{fc}, $|Xc|_{max}$ and $|Z|_{fc}$, as well as their respective average and

Table 2. Simulated values of biological parameters

Patient code	$\|Z\|_{100Hz}$ (Ω)	R_{100Hz} (Ω)	$\|X_c\|_{100Hz}$ (Ω)	$\|\theta\|_{100Hz}$ (°)	$\|Z\|_{10GHz}$ (Ω)	R_{10GHz} (Ω)	$\|X_c\|_{10GHz}$ (Ω)	$\|\theta\|_{10GHz}$ (°)
1	433	433	0.09	0.01	369	369	0.48	0.07
2	459	459	0.23	0.03	362	362	0.40	0.06
3	667	667	0.24	0.02	569	569	0.40	0.04
4	520	520	0.22	0.02	426	426	0.40	0.05
5	500	500	0.08	0.01	454	454	0.25	0.03
6	600	600	0.32	0.03	472	472	0.52	0.06
7	515	515	0.28	0.03	397	397	0.50	0.07
8	652	652	0.37	0.03	503	503	0.60	0.07
9	638	638	0.34	0.03	509	509	0.48	0.05
10	789	789	0.41	0.03	664	664	0.38	0.03
11	676	676	0.30	0.03	566	566	0.41	0.04
12	466	466	0.23	0.03	368	368	0.42	0.06
13	663	663	0.23	0.02	553	553	0.54	0.06
14	599	599	0.30	0.03	462	462	0.63	0.08
15	648	648	0.34	0.03	513	513	0.54	0.06
16	443	443	0.13	0.02	362	362	0.40	0.06
17	437	437	0.09	0.01	367	367	0.55	0.09
18	762	762	0.32	0.02	633	633	0.52	0.05
19	598	598	0.16	0.02	521	521	0.37	0.04
20	761	761	0.33	0.02	634	634	0.50	0.04
21	641	641	0.37	0.03	501	501	0.53	0.06
22	612	612	0.04	0.00	573	573	0.35	0.04
23	463	463	0.11	0.01	413	413	0.22	0.03
Average	588.0	588.3	0.25	0.02	486.6	486.6	0.46	0.05
Standard deviation	110.8	110.8	0.11	0.01	94.1	94.1	0.10	0.02

Note: $|Z|_{100\,Hz}$, $R_{100\,Hz}$, $|X_c|_{100\,Hz}$, $|\theta|_{100\,Hz}$, $|Z|_{10\,GHz}$, $R_{10\,GHz}$, $|X_c|_{10\,GHz}$ and $|\theta|_{10\,GHz}$ were defined in methods section.

SD for each NDLCAPs. This table reveals that Ri values were higher than those of for each NDLCAPs. The average value of was near to 50 kHz; nevertheless, 18 NDLCAPs (codes 2-4, 6-15, 18-21 and 23) and five NDLCAPs (codes 1, 5, 16, 17 and 22) had values of below and above 50 kHz, respectively. No anomalous behavior was observed in |Z| for each NDLCAPs when the value of |Z|fc was introduced into the experimental data, keeping in mind whether fc was below/above 50 kHz, which was referenced for two reasons. First, 50 kHz was frequently used in clinics. (1) Second, in HAASs was close to 50 kHz. The average ± SD of Re, Ri, Cm, fc, Rfc, |Xc|max and Rfc in men NDLCAPs were 537.8 ± 107.7 Ω, 2 661.9 ± 1 007.3 Ω, 1.69 ± 1.90 nF, 48.7 ± 13.3 kHz, 48.5 ± 16.4 Ω and 489.3 ± 96.7 Ω, respectively. The respective values of these six bioelectrical parameters for women were 667.0 ± 58.7 Ω, 3 911.1 ± 2022.5 Ω, 0.90 ± 0.33 nF, 45.7 ± 16.9 kHz, 54.7 ± 16.6 Ω and 612.3 ± 52.5 Ω. This analysis by gender revealed that average values of R_e, R_i, f_c, |Xc|max and Rfc in women NDLCAPs were higher than those in men NDLCAPs. Furthermore, average value of in men NDLCAPs was higher than that in women NDLCAPs. High variability in SD for was observed for both genders, being bigger in women NDLCAPs.

DISCUSSION

Although the frequency sweep range is varied from Hz

Table 3. Values of $|Z|_{exp}$, $|Z|_{sim}$, and $\Delta|Z|$ and RMS $\Delta|Z|$

Patient code	Values of $\|Z\|$												$RMS_{\Delta\|Z\|}$ (Ω)
	5 kHz			50 kHz			100 kHz			200 kHz			
	(Ω)	(Ω)	(Ω)	(Ω)	(Ω)	(Ω)	(Ω)	(Ω)	(Ω)	(Ω)	(Ω)	(Ω)	
1	433	432.7	-0.3	416	414.2	-1.8	391	393.1	2.1	369	377.4	8.4	4.4
2	459	457.7	-1.3	404	404.2	0.2	382	377.7	-4.3	362	366.5	4.5	3.2
3	667	665.7	-1.3	611	610.6	-0.4	588	584.3	-3.7	569	573.3	4.3	2.9
4	520	518.8	-1.2	467	467.3	0.3	444	441.4	-2.6	426	430.4	4.4	2.6
5	500	499.6	-0.4	479	479.5	0.5	467	464.9	-2.1	454	457.3	3.3	2.0
6	600	598.3	-1.7	526	526.6	0.6	496	492.1	-3.9	472	477.7	5.7	3.6
7	515	513.6	-1.4	446	450.0	4.0	531	417.1	-113.9	397	402.8	5.8	57.1
8	652	559.9	-1.9	565	501.0	-64.0	528	482.1	-45.9	503	475.3	-27.7	41.8
9	638	636.0	-2.0	559	558.9	-0.1	664	513.9	-150.1	509	513.9	4.9	75.1
10	789	786.0	-3.0	696	700.0	4.0	578	675.5	97.5	664	667.1	3.1	48.8
11	676	674.2	-1.8	601	607.2	6.2	393	580.3	187.3	566	570.0	4.0	93.7
12	466	464.8	-1.2	412	411.6	-0.4	578	373.0	-205	368	372.8	4.8	102.5
13	663	661.9	-1.1	609	609.0	0.0	494	575.7	81.7	553	559.7	6.7	41.0
14	599	597.6	-1.4	524	529.3	5.3	538	488.7	-49.3	462	569.9	107.9	59.4
15	648	646.1	-1.9	569	569.0	0.0	382	533.4	151.4	513	518.7	5.7	75.8
16	433	432.5	-0.5	403	403.0	0.0	393	380.1	-12.9	362	367.6	5.6	7.0
17	437	436.7	-0.3	418	418.0	0.0	657	395.1	-261.9	367	377.1	10.1	131.0
18	762	760.2	-1.8	687	687.0	0.0	540	652.7	112.7	633	638.6	5.6	56.4
19	598	597.2	-0.8	560	559.3	-0.7	657	536.3	-120.7	521	525.5	4.5	60.4
20	761	759.1	-1.9	688	684.9	-3.1	531	652.2	121.2	634	639.1	5.1	60.7
21	641	638.9	-2.1	561	556.4	-4.6	589	520.8	-68.2	501	506.5	5.5	34.3
22	612	611.9	-0.1	603	603.0	0.0	419	590.7	171.7	573	579.7	6.7	85.9
23	463	462.4	-0.6	436	436.0	0.0	420	321.8	-98.2	413	415.5	2.5	49.1
Average	584.0	583.1	-1.3	532.2	529.8	-2.3	507.0	497.5	-9.4	486.6	494.9	8.3	-
Standard deviation	110.0	109.5	-0.5	95.3	95.3	0.0[1]	92.6	99.9	7.3	94.1	94.9	0.8	-

Note: $|Z|_{exp}$, $|Z|_{sim}$, and $\Delta|Z|$ and RMS $\Delta|Z|$ were defined in methods section.

to MHz/GHz in several multifrequency BIA analyzers to characterize AHASs and patients with different pathologies, the results of this study suggest that electrical characterization in NDLCAPs is sufficient up to 200 kHz, in agreement with the recommendations of the manufacturer of this BIA analyzer. [19,20,21] The increase in |Z|, Δ|Z|| > 10 Ω and RMS Δ|Z| > 10 Ω at 100 and 200 kHz observed in 14 NDLCAPs (60.9% = 14/23) contrasts with theory, which predicts that |Z| decreases as frequency increases because Re and Ri do not change with frequency and |Xc| is inversely proportional to frequency. This anomalous behavior at 100 and 200 kHz may explain deformation of the semicircle in |Xc| versus plot for $f > f_c$ and therefore experimental data do not strictly follow the Cole-Cole function distribution in the majority of these NDLCAPs (73.9% = 17/23), in agreement with other studies. [19] This finding may be explained by different reasons. First, the β-dispersion itself (tens of kHz to tens of MHz) is due to tissues with multiple relaxations (multiple β-dispersions) in NDLCAPs depending on the number of compartments considered in them, each with different biological characteristics, Warburg diffusion, metabolisms, electrical properties and bioelectricity. [6,8] Therefore, the electrical equivalent circuit shown in figure 1b would be more complex because it would have two (two β-dispersions) or more (multiple β-disper-

Table 4. Values of R_e, R_i, C_m, f_c, R_{fc}, $|Xc|_{max}$, R_{fc} and $|Z|_{fc}$

Patient code	R_e (Ω)	R_i (Ω)	C_m (nF)	f_c (kHz)	$\|X_c\|_{max}$ (Ω)	R_{fc} (Ω)	$\|Z\|_{fc}$ (Ω)
1	433	2497	0.73	74.6	32.0	401.0	402
2	459	1713	1.77	41.3	48.5	410.5	413
3	667	3873	0.85	41.3	49.0	618.0	620
4	520	2357	1.31	42.1	47.0	473.0	475
5	500	4935	0.54	54.4	23.0	477.0	478
6	600	2213	1.39	40.6	64.0	536.0	540
7	515	1733	1.67	42.3	59.0	456.0	460
8	652	2201	1.39	40.1	74.5	577.5	582
9	638	2517	1.34	37.5	64.5	573.5	577
10	789	4191	1.05	30.5	62.5	726.5	729
11	676	3478	1.04	37.0	55.0	621.0	623
12	466	1750	1.69	42.5	49.0	417.0	420
13	663	3333	8.18	48.7	55.0	608.0	610
14	599	2020	1.32	46.0	68.5	530.5	535
15	648	2462	1.29	39.7	67.5	580.5	584
16	433	2208	1.08	55.9	35.5	397.5	399
17	437	2291	0.74	78.5	35.0	402.0	404
18	762	3739	0.87	40.5	64.5	697.5	700
19	598	4046	0.71	48.1	38.5	559.5	561
20	761	3799	0.89	39.1	63.5	697.5	700
21	641	2294	0.89	38.0	70.0	571.0	575
22	612	8992	0.18	89.8	19.5	592.5	593
23	463	3824	0.83	44.8	25.0	438.0	439
Average	588.0	3150.7	1.4	47.5	50.9	537.5	540.0
Standard deviation	110.8	1573.4	1.5	14.5	16.4	101.4	101.6

Note: R_e, R_i, C_m, f_c, R_{fc}, $|Xc|_{max}$, R_{fc} and $|Z|_{fc}$ were defined in methods section.

sions) RC branches in parallel, each of them with a characteristic time constant. Consequently, two or multiple arches would appear in the |Xc| versus R plot that would result from the superposition of two or multiple differentiated relaxation processes, in agreement with other authors. [22]

Second, tissues in NDLCAPs may simultaneously show two different dispersion types because the end of α-dispersion $f \leq 100$ Hz) overlaps β-dispersion (range 100 Hz-1 MHz). [22] The α-dispersion (due to ionic diffusion phenomena of the ions that surround the cell membrane) should not be discarded since the diffusion of ions through cancer cell membranes is permanently altered due to its permanent depolarization and the anomalous diffusion of ions (ionic current) and electrons (faradic current) in cancer (differs markedly from that in the surrounding healthy tissue) that may lead to electrolyte imbalance and anomalous redistribution of body water in its compartments. [1,7,6,8,23]

The third reason, normal and cancer tissues are fractal in nature because they are considered as fractional-order systems. [24,25,26] Therefore, fractional order impedance modeling and fractional-order circuit models may be used to characterize dynamic of these tissues to describe best averaged data respect to integer-order circuit models, in agreement with Freebom et al. [22] This may suggest that values of *R*, |*Xc*|, |*Z*|, R_e, R_i and in NDLCAPs may be fractions and not integers for any value of ; therefore, NDLCAPs may be considered as an equivalent network formed by electric circuit elements with fractional order impedance depending on biological characteristics and electrical properties of cancer and surrounding healthy tissue; the performance status and concomitant pathologies of them, and existence or not metastasis in these patients.

The 14 NDLCAPs who show anomalous behaviors of |*Z*| at 100 or 200 kHz correspond to those with sarcopenia (codes 4, 5, 8, 13 and 18), type 2 diabetes (codes 1, 4, 9, 10, 11, 12 and 17), marked pleural effusion in the entire left lung (codes 8 and 17), dehydration due to the diarrhea (code 14 consumes Sildenafil), decrease in (codes 4, 5, 6, 8, 13, 14, 15, 16, 19 and 20). Furthermore d-ECOG 3 and adenocarcinoma (57.1% = 8/14), stages IIIB and IV (85.7% =12/14) and f_c < 50 kHz (85.7% = 12/14) may influence on these anomalous behaviors. These aspects may change also *R*, |*Xc*|, |*Z*|, |*θ*|, R_e, R_i and Cm values in NDLCAPs, in agreement with other studies in cancer. [3,23]

In NDLCAPs, Ri >>Re may be interpreted as the intracellular fluid is less conductive than the extracellular fluid in cancer cells. Thus, intratumor water is mainly concentrated on the extracellular fluids of cancer cells, which may be related to the electrolyte imbalance in LCPs and why the water concentration is higher in the tumor than in the surrounding healthy tissue, in agreement with. [1] It is expected that water is primarily concentrated in the intracellular fluids (R_i << R_e) of cancer cells because this is physiological in normal cells, in addition to the high concentration of sodium ions in their intracellular fluids, by their low transmembrane potentials, which are related to permanent depolarization and failure of ionic pumps (mainly sodium/potassium pump) in their cellular membranes, depletion of adenosine triphosphate in these cells, among others. [7,27,1] These alterations and others may suggest that NDLCAPs requires more time to return from its disturbed state (presence of the lung cancer) to the base state (absence of the lung cancer, as in AHASs). [28,29] Consequently, relaxation time in them is longer; therefore, decreases. This may explain, in part, why most NDLCAPs (78.3% = 18/23) have fc < 50 kHz. If these alterations in NDLCAPs are marked over time, deterioration of their organisms is expected, as in untreated mice bearing tumor (control groups). [28]

Alterations in cancer patients (14 hallmarks of cancer) are related to bioelectricity in cancer and surrounding healthy tissue, which differ from each other, and generation of electrical energy in cells (triboelectric nanogenerators). [6,8,30,31,32] Biological and bioelectrical alterations in NDLCAPs may explain why experimental data do not follow a Cole-Cole distribution function for α = 1. [1,6,8,28,29,33,34] Consequently, the Cole-Cole distribution function for 0 < α < 1 or another distribution function (e.g., Havriliak- Negami, Cole-Davidson or Warburg relaxation model) may be used by means of two ways. First, the geometric analysis for each distribution function (arcs in |*Xc*| versus R plot), keeping in mind values of |Z| at 5, 50, 100 and 200 kHz. [35] Second, the use of multifrequency device (e.g., MultiScan® 5000 BIS at 50 frequencies in the range 5 kHz-1 000 kHz, which has implemented the Havriliak-Negami distribution function. [36] Furthermore, anomalies in NDLCAPs for *f* > *fc* may be explained because they may behave like fractal antennas since cancer and normal tissues are considered as fractals, and fractional-order system, the whole-human body is considered as a multi-faceted antenna system with different resonant frequencies and natural resonant frequencies of cancerous tissues differ completely from those of healthy tissues. [24,25,37,38,39] Consequently, these patients may be considered as multi-resonance systems (several resonance frequencies), keeping in mind that fractal antennas are multi-resonance systems too. [40]

The beforementioned aspects have not been integrated or related to bioelectrical parameters of cancer and normal tissues in the literature. The possible existence of multi-resonance frequencies in NDLCAPs may suggest the presence of inductive elements (e.g., iron in the heme group in blood and in deoxyribonucleic acid) in these patients. [16] Three possibilities may be possible: a) in figure 1B, add the inductive element in series with Ri and Cm in a branch, which is in parallel with R_e. b) in figure 1B, add the inductive element in series with Re in a branch, which is in parallel with the branch that contains R_i and C_m in series. c) in figure 1B, add the inductive element in series with R_i and C_m in a branch, which is in parallel with another branch that contains other inductive element in series with R_e. In general, these two inductive elements are different. A further study will be carried out to elucidate which of these three possibilities best describes experimental data. These three possibilities should not be confused with inductive element in a branch, which is in parallel with branch of Re and branch of R_i and Cm connected in series reported in. [16]

As biological systems are nonlinear, NDLCAPs were chosen because knowledge of their initial conditions (*R*, |*Xc*|, |*Z*|, |*θ*|, R_e, R_i and C_m values) is vital for their prognoses without and with the application of anticancer therapy. This latter may be verified in a future longitudinal study. This requires that the BIA should not be used only to know the averages ± SD of the bioelectrical and biological parameters in a population of NDLCAPs, but also for the individual analysis of each of them. This is essential for understanding of biophysical individuality of each of these patients and the selection of personalized/individualized anticancer therapies for each NDLCAPS.

Conclusions

The bioelectrical impedance analysis reveals anomalous behaviors of bioelectrical parameters in each newly diagnosed lung cancer adult patients for frequencies above characteristic frequency. These behaviors may be described by Cole-Cole distribution functions (for 0 < α < 1) or others.

REFERENCES

1. Regüeiferos JCC, Luna TTB, Brooks SCA, Rodríguez MP, Zamora-Matamoros L, Legrá-Rodríguez B, Fernández AP, Bello JLG, Montoya-Pedrón A, González MM, Garcia JCN, Cascaret-Fonseca E, Cabrales LEB. Integrated analysis of clinical, bioelectrical and functional variables in newly diagnosed lung cancer adult patients: pilot study. Translational Medicine Communications, 2022 [citado 15 oct 2023];7:1. https://doi.org/10.1186/s41231-022-00127-3
2. Hui D, Dev R, Pimental L, Park M, Cerana MA, Liu D, Bruera E. Association between multi-frequency phase angle and survival in patients with advanced cancer. Journal Pain Symptom Manage, 2017 [citado 15 oct 2023];53(3):571-77. https://doi.org/10.1016/j.jpainsymman.2016.09.016
3. Toso S, Piccoli A, Gusella M, Menon D, Bononi A, Crepaldi G, Ferrazi E. Altered tissue electric properties in lung cancer patients as detected by bioelectric impedance vector analysis. Nutrition, 2000 [citado 15 oct 2023];16(2):120-124. https://doi.org/10.1016/S0899-9007(99)00230-0
4. Sasaki K, Porter E, Rashed EA, Farrugia L, Schmid G. Measurement and image-based estimation of dielectric properties of biological tissues-past, present, and future. Physics in Medicine & Biology, 2022 [citado 23 mar 2024];67(14). https://doi.org/10.1088/1361-6560/ac7b64
5. Di Meo S, Bonello J, Farhat I, Farrugia L, Pasian M, Camilleri-Podesta MT. The variability of dielectric permittivity of biological tissues with water content. Journal Electromagnetics Waves and Applications, 2022 [citado 23 mar 3024];36(1):48-68. https://doi.org/10.1080/09205071.2021.1956375
6. Robinson J, Jain A, Sherman H, Hague R, Rahman R, Sanjuan-Alberte P, Rawson F. Toward hijacking bioelectricity in cancer to develop new bioelectronic medicine. Advanced Therapeutics, 2021 [citado 23 mar 2024];4(3). https://doi.org/10.1002/adtp.202000248
7. Bory-Prevez H, Soutelo-Jiménez AA, Roca-Oria EJ, Heredia-Kindelán JA, Morales-González M, Villar-Goris NA, Hernández-Mesa N, Sierra-González VG, Infentaes-Frómeta Y, Montijano JI, Bergues-Cabrales LE. Simulations of surface charge density changes during the untreated solid tumor growth. Royal Society Open Science, 2022 [citado 05 oct 2024];9(11):220552. https://doi.org/10.1098/rsos.220552
8. Singh K, Awasthi R, Malviya RR. Bioelectronic medicines: Therapeutic potential and advancements in next-generation cancer therapy. Biochimica et Biophysica. Acta (BBA) Reviews on Cancer, 2022 [citado 05 oct 2024];1877(6):188808. https://doi.org/10.1016/j.bbcan.2022.188808
9. Dahlmann N, Demond V. A new anthropometric model for body composition estimation: Comparison with a bioelectrical impedance consumer device. Plos One, 2022 [citado 15 oct 2023];17(9):e0271880. https://doi.org/10.1371/journal.pone.0271880
10. Morlino D, Cioffi I, Marra M, Di Vincenzo O, Scalfi L, Pasanisi F. Bioelectrical phase angle in patients with breast cancer: a systematic review. Cancers (Basel), 2022 [citado 23 mar 2024];14(8):2002. https://doi.org/10.3390/cancers14082002
11. Praget-Bracamontes S, González-Arellanes R, Aguilar-Salinas CA, Martagón AJ. Phase angle as a potential screening tool in adults with metabolic diseases in clinical practice: A systematic review. International Journal of Environmental Research and Public Health, 2023 [citado 23 mar 2024]; 20(2):1608. https://doi.org/10.3390/ijerph20021608
12. Nieto-Villar JM, Mansilla R. Longevity, aging and cancer: Thermodynamics and complexity. Foundations, 2022 [citado 15 oct 2023];2:664. https://doi.org/10.13133/2532-5876/17613
13. Lucia U, Grisolia G. Thermal resonance in living cells to control their heat exchange: Possible applications in cancer treatment. International Communications in Heat and Mass Transfer, 2022 [citado 04 nov 2024];131:105842. https://doi.org/10.1016/j.icheatmasstransfer.2021.105842
14. WMA Declaration of Helsinki–Ethical Principles for Medical Research Involving Human Subjects. 64th WMA General Assembly, Fortaleza, Brazil, October 2013. Disponible en: https://www.wma.net/policies-post/wma-declaration-of-helsinki-ethical-principles-for-medical-research-involving-human-subjects/
15. Buenas Prácticas Clínicas en Cuba, Centro para el Control Estatal de la Calidad de los Medicamentos (CECMED), La Habana, Cuba, (2000), Disponible en: https://www.google.com/url?sa=t&rct=j&q=&esrc=s&source=web&cd=&ved=2ahUKEwiIxfLsk9vxAhXVTjABHdYjBMYQFjAAegQIBxAD&url=https%3A%2F%2Fwww.cecmed.cu%2Ffile%2F1984%2Fdownload%3Ftoken%3DOeQm92f3&usg=AOvVaw2KRGkA8C5KqWnfmDlytS25
16. Lafargue AL, Cabrales LEB, Larramendi RM. Inductance of body tissues obtained by bioelectrical impedance analysis method. Bioelectromagnetics, 2002 [citado 23 abr 2024];23:450. https://doi.org/10.1002/bem.10034
17. Nescolarde L, Núñez A, Bogónez-Franco P, Lara A, Vaillant G, Morales R, Rosell-Ferrer J. Reference values of the bioimpedance vector components in a Caribbean population. e-SPEN J, 2013 [citado 05 sep 2024];8(4):e141-e144. https://doi.org/10.1016/j.clnme.2013.04.004
18. Cole KS, Cole RH. Dispersion and absorption in dielectrics II. Direct current characteristics. Journal of Chemical Physics, 1942 [citado 03 nov 2024];10:98. https://doi.org/10.1063/1.1723677
19. Moqadam SM, Grewal PK, Haeri Z, Ingledew PA, Kohli K, Golnaraghi F. Cancer detection based on electrical impedance spectroscopy: A clinical study. Journal of Electrical Bioimpedance, 2018 [citado 12 feb 2024];9(1):17-23. https://doi.org/10.2478/joeb-2018-0004
20. Freeborn TJ, Elwakil AS, Maundy B. Compact wide frequency range fractional-order models of human body impedance against contact currents. Mathematical Problems in Engineering, 2016 [citado 17 may 2024];2016(1):4967937. https://doi.org/10.1155/2016/4967937
21. Sipers WM, Dorge J, Schols JM, Verdijk LB, Van Loon LJ. Multifrequency bioelectrical impedance analysis may represent a reproducible and practical tool to assess skeletal muscle mass in euvolemic acutely ill hospitalized geriatric patients. European Geriatric Medicine, 2020 [citado 03 ene 2024];11(1):155-162. https://doi.org/10.1007/s41999-019-00253-6
22. Osypka M, Gersing E. Tissue impedance spectra and the appropriate frequencies for EIT. Physiological Measurement, 1995 [citado 14 jun 2024];16(3A):A49. https://doi.or-

g/10.1088/0967-3334/16/3A/005

23. Nwosu AC, Mayland CR, Mason S, Cox TF, Varro A, Ellershaw J. The association of hydration status with physical signs, symptoms and survival in advanced cancer-The use of bioelectrical impedance vector analysis (BIVA) technology to evaluate fluid volume in palliative care: an observational study. Plos One, 2016 [citado 14 jul 2024];11(9):e0163114. https://doi.org/10.1371/journal.pone.0163114
24. Elkington L, Adhikari P, Pradhan P. Fractal dimension analysis to detect the progress of cancer using transmission optical microscopy. Biophysica, 2022 [citado 10 sep 2024];2(1):59-69. https://doi.org/10.3390/biophysica2010005
25. Sahu T, Tripathy MC, Sahoo SP. An intelligent fractional-order system for the biological parameters regulations. International Journal of Dynamics and Control, 2022 [citado 27 jun 2024];11(4):1880. https://doi.org/10.1007/s40435-022-01088-z
26. Ghita M, Copot D, Ionescu CM. Lung cancer dynamics using fractional order impedance modeling on a mimicked lung tumor setup. Journal of Advanced Research, 2021 [citado 14 sep 2024];32:61-71. https://doi.org/10.1016/j.jare.2020.12.016
27. Leslie TK, Brackenbury WJ. Sodium channels and the ionic microenvironment of breast tumours. Journal of Physiology, 2023 [citado 07 nov 2024];601(9):1543-1553. https://doi.org/10.1113/JP282306
28. Morales-González M, González-Joa JA, Bergues-Cabrales LE, Bergues-Pupo AE, Schneider B, Kondakci S, Camué-Ciria HM, Bory-Reyes J, Verdecia-jarque M, O´farril-Mateus MA, Rubio-González T, Acosta-Brooks SC, Hernández-Cáceres JL, Sierra-González GV. Is cancer a pure growth curve or does it follow a kinetics of dynamical structural transformation? BMC Cancer, 2017 [citado 11 dic 2024];17:1-14. https://doi.org/10.1186/s12885-017-3159-y
29. Hanahan D. Hallmarks of cancer: new dimensions. Cancer Discovery, 2022 [citado 13 dic 2024];12(1):31. https://doi.org/10.1158/2159-8290.CD-21-1059
30. Sheth M, Esfandiari L. Bioelectric dysregulation in cancer initiation, promotion, and progression. Frontiers in Oncology, 2022 [citado 04 dic 2024];12:846917. https://doi.org/10.3389/fonc.2022.846917
31. Levin M. Bioelectrical approaches to cancer as a problem of the scaling of the cellular self. Progress in Biophysics and Molecular Biology, 2021 [citado 25 jun 2024];165:102. https://doi.org/10.1016/j.pbiomolbio.2021.04.007
32. Zhang W, Wang B, Zhu Q, Li G. Triboelectric nanogenerators for cellular bioelectrical stimulation. Advanced Functional Materials, 2022 [citado 09 jul 2023];32(34):2203029. https://doi.org/10.1002/adfm.202203029
33. Di Gregorio E, Israel S, Staelens M, Tankel G, Shankar K, Tuszyński JA. The distinguishing electrical properties of cancer cells. Physics of Life Reviews, 2022 [citado 21 ene 2025];43:139-188. https://doi.org/10.1016/j.10.1016/j.plrev.2023.08.003plrev.2022.09.003
34. Kim SJ, Khadka D, Seo JH. Interplay between solid tumors and tumor microenvironment. Frontiers in Immunology, 2022 [citado 26 ago 2024];13:882718. https://doi.org/10.3389/fimmu.2022.882718
35. Elwakil AS, Al-Ali AA, Maundy BJ. Extending the double-dispersion Cole-Cole, Cole-Davidson and Havriliak-Negami electrochemical impedance spectroscopy models. European Biophysics Journal, 2021 [citado 23 ene 2025];50(6):915-926. https://doi.org/10.1007/s00249-021-01545-1
36. Lee SW, Ying CL, Ruey H, Haroon S, Kin WW, Jc Lee E, WL Lau T, Sethi S, Wee B. Evaluation of different bioimpedance methods for assessing body composition in Asian non-dialysis chronic kidney disease patients. Kidney Research and Clinical Practice, 2019 [citado 11 mar 2025];38(1):71-80. https://doi.org/10.23876/j.krcp.18.0069
37. Kibret B, Teshome AK, Lai D. Human body as antenna and its effect on human body communications. Progress in Electromagnetics Research, 2014 [citado 13 feb 2025];148:193-207. https://doi.org/10.2528/PIER14061207
38. J. M. Randall, R. T. Matthews, and M. A. Stiles, Resonant frequencies of standing humans. Ergonomics, 1997 [citado 11 mar 2025];40(9):879-886. https://doi.org/10.1080/001401397187711
39. Calabrò E, Magazù S. New perspectives in the treatment of tumor cells by electromagnetic radiation at resonance frequencies in cellular membrane channels. The Open Biotechnology Journal, 2019 [citado 17 feb 2025];13(1):105-110. https://doi.org/10.2174/187407070190130105
40. Zhou E, Cheng Y, Chen F, Luo H, Li X. Low-profile high-gain wideband multi-resonance microstrip-fed slot antenna with anisotropic metasurface. Progress in Electromagnetics Research, 2022 [citado 25 mar 2025];175:91-104. https://doi.org/10.2528/pier22062201

Received: 14/04/2025
Aproved: 6/02/2026

Acknowledgements

The authors thank to Josué Mariño Del Pozo, Zuzel Idalia Fernández Rodríguez and Antonio Rafael Selva Castañeda (Universidad de Oriente, Santiago de Cuba) for their useful comments. We appreciate the valuable comments from the anonymous reviewers and the editorial board of AACC journal. Furthermore, the authors appreciate the help received of the paramedical staff of the Hospital General Dr. Juan Bruno Zayas Alfonso and the professors of Universidad de Ciencias Médicas de Santiago de Cuba, Cuba. This research is supported by the Hospital Clínico Quirúrgico Juan Bruno Zayas, Santiago de Cuba, Cuba [grant number: 108823SC-900-149 (2018-2021)].

Competing interests

The authors declare that there are no conflicts of interest among them or with the research presented.

Authors' contributions

- Conceptualization: Dunia Rodríguez-Heredia, Henry Bory-Prevez, Luis Enrique Bergues Cabrales
- Data curation: Dunia Rodríguez-Heredia, Arnolis Poll-Fernández, Maylet Planas-Rodríguez, Henry Bory-Prevez, Justa Carmen Columbié-Regüeiferos, Luis Enrique Bergues Cabrales
- Formal analysis: Dunia Rodríguez-Heredia, Arnolis Poll-Fernández, Maylet Planas-Rodríguez, Henry Bory-Prevez, Justa Carmen Columbié-Regüeiferos, Luis Enrique Bergues Cabrales
- Research: Dunia Rodríguez-Heredia, Arnolis Poll-Fernández, Maylet Planas-Rodríguez, Henry Bory-Prevez, Justa Carmen

Columbié-Regüeiferos, Luis Enrique Bergues Cabrales

- Metodology: Dunia Rodríguez-Heredia, Henry Bory-Prevez, Justa Carmen Columbié-Regüeiferos, Luis Enrique Bergues Cabrales
- Project management: Justa Carmen Columbié-Regüeiferos
- *Software*: Henry Bory-Prevez
- Validation: Luis Enrique Bergues Cabrales
- Display: Dunia Rodríguez-Heredia, Arnolis Poll-Fernández, Maylet Planas-Rodríguez, Henry Bory-Prevez, Justa Carmen Columbié-Regüeiferos, Luis Enrique Bergues Cabrales
- Writing-original draft: Dunia Rodríguez-Heredia, Henry Bory-Prevez, Luis Enrique Bergues Cabrales
- Writing-review and editing: Dunia Rodríguez-Heredia, Arnolis Poll-Fernández, Maylet Planas-Rodríguez, Henry Bory-Prevez, Justa Carmen Columbié-Regüeiferos, Luis Enrique Bergues Cabrales

Fundings

This study is supported by Hospital General Juan Bruno Zayas de Santiago de Cuba, Cuba (grant PI-108823SC-900-149).

How to cite this article

Rodríguez-Heredia D, Poll-Fernández A, Planas-Rodríguez M, Bory-Prevez H, Columbié-Regüeiferos JC, Bergues Cabrales LE. Bioelectrical parameters estimated in newly diagnosed lung cancer patients with multifrequency-bioelectrical impedance. An Acad Cienc Cuba [internet] 2025 [citado en día, mes y año];15(4):e3042. Disponible en: http://www.revistaccuba.cu/index.php/revacc/article/view/3042